Organic & Biomolecular Chemistry

www.rsc.org/obc

Volume 8 | Number 19 | 7 October 2010 | Pages 4185–4484

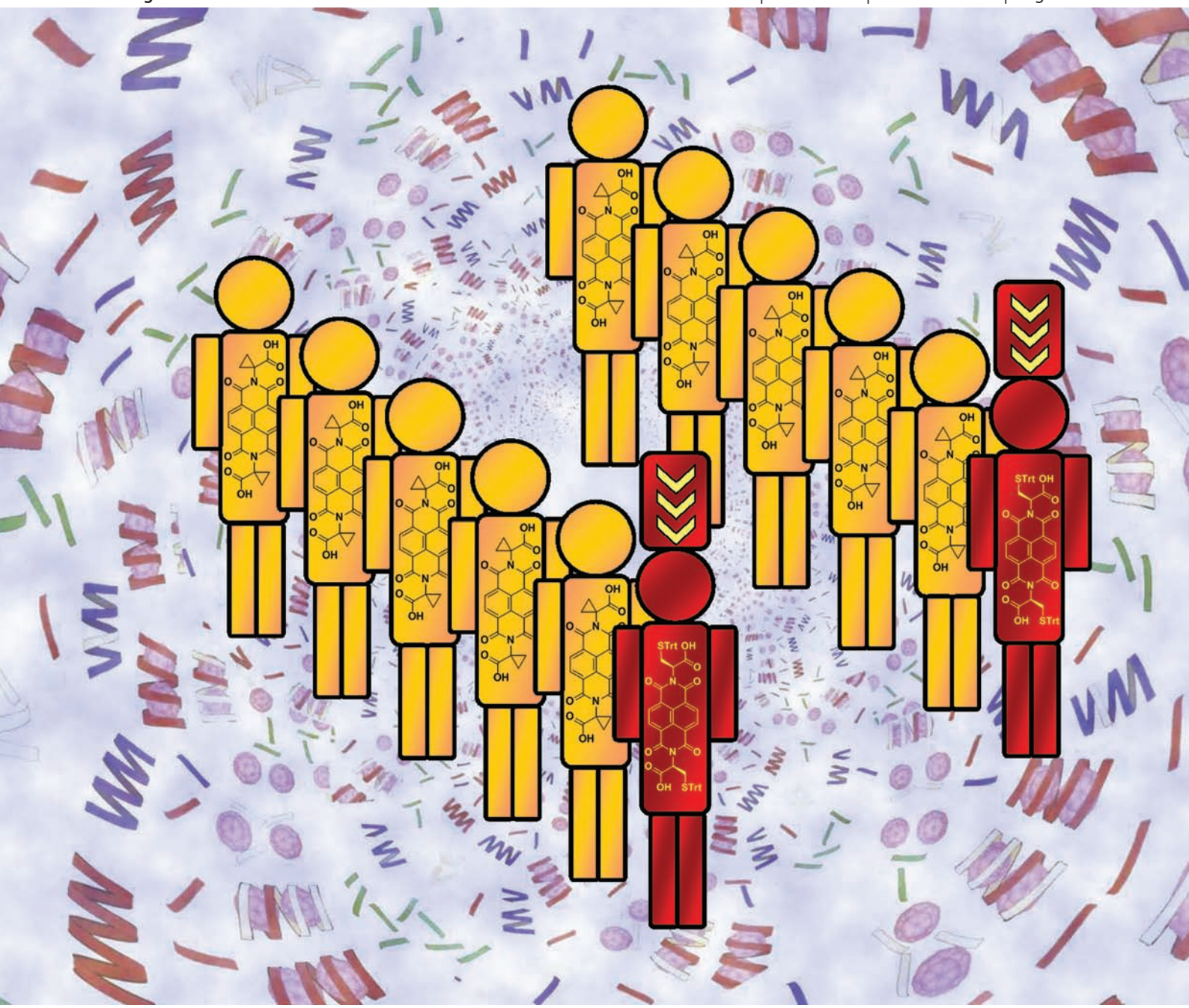

ISSN 1477-0520

RSC Publishing

FULL PAPER
Tom W. Anderson *et al.*
The sergeants-and-soldiers effect: chiral amplification in naphthalenediimide nanotubes

EMERGING AREA
Lalla Aicha Ba *et al.*
Tellurium: an element with great biological potency and potential

1477-0520(2010)8:19;1-V

The sergeants-and-soldiers effect: chiral amplification in naphthalenediimide nanotubes†

Tom W. Anderson, Jeremy K. M. Sanders and G. Dan Pantoş*

Received 21st April 2010, Accepted 9th June 2010
DOI: 10.1039/c0ob00027b

Self-assembling naphthalenediimide (NDI)-based helical organic nanotubes display sergeants-and-soldiers behaviour, chiral monomers imposing a supramolecular structure upon achiral monomers. Several achiral NDI monomers were synthesised and their ability to incorporate into supramolecular nanotubes was studied. Nanotubes containing predominantly the most effective soldier, derived from 1-aminocyclopropane-carboxylic acid, are effective hosts for C_{60}.

Introduction

We report here that achiral building blocks can be incorporated into chiral helical nanotubes, exhibiting 'sergeants-and-soldiers' organisation[1] as judged by both spectroscopic and functional binding behaviour. Many chiral amino acid derivatives of naphthalenediimides (NDIs) may be readily obtained in good yield by the microwave reaction of the relevant amino acid with naphthalene dianhydride (NDA), as shown in Scheme 1.[2] These molecules were found to spontaneously self-assemble into helical nanotubes when dissolved in an aprotic solvent such as chloroform.[3]

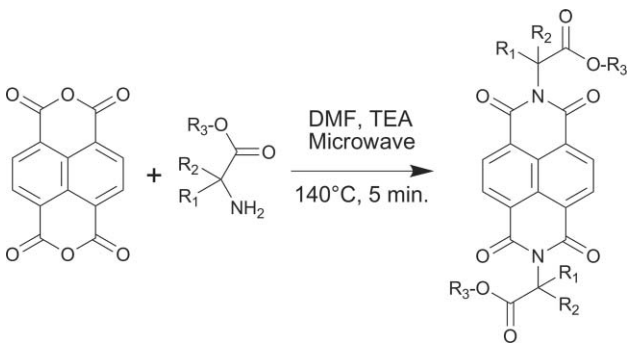

Scheme 1 Generalised microwave synthesis of NDIs from NDA and amino acids (or esters). For more details, such as the range of R-groups employed, see ref. 2

This assembly is due to two sets of hydrogen bonds. Firstly, a classical O–H···O interaction between the carboxylic acid-functionalised ends of each NDI monomer produces a supramolecular polymer. Secondly, a non-classical C–H···O interaction between an aromatic hydrogen of the naphthyl core and a diimide carbonyl oxygen, specifically between NDI *i* and *i* + 3 (see Fig. 1), is responsible for aligning the NDI cores to be coplanar.

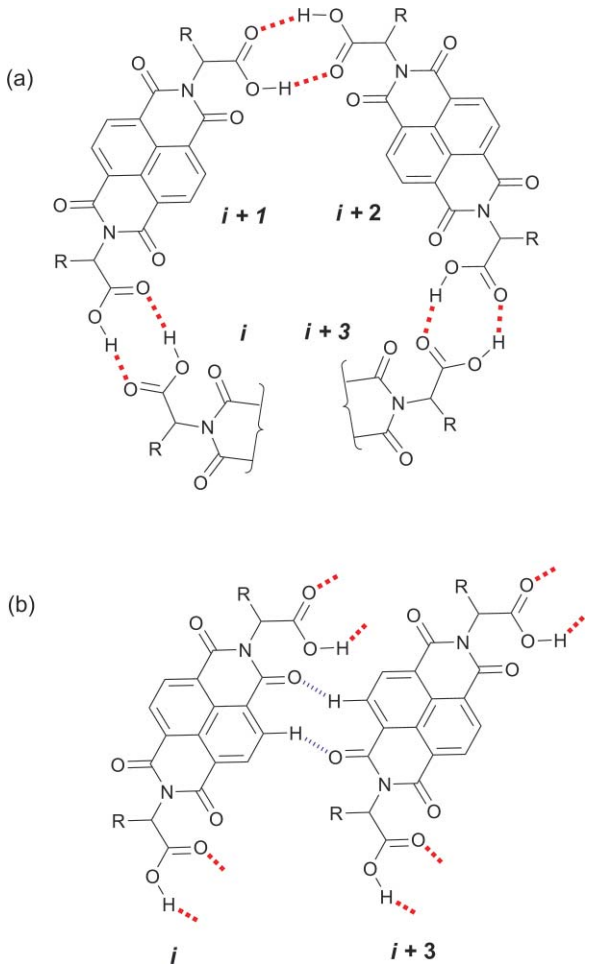

Fig. 1 Brief overview of the two forms of hydrogen bonding in the NDI nanotubes: (a) the classical O–H···O carboxylic acid dimerisation and (b) the non-classical C–H···O cross-bonding between NDI *i* and *i* + 3 (immediately below it in the helix).[3]

The presence of these two types of hydrogen bonding along with the amino acid chiral centre impose a helical twist to the structure, meaning that this is not simply a linear supramolecular polymer, but a supramolecular nanotube. This structure resulting from hydrogen-bond-directed assembly is preferred in this case over the more usual π–π stacking geometry.[4,5]

University Chemical Laboratory, University of Cambridge, Lensfield Road, Cambridge, UK CB2 1EW. E-mail: gdp26@cam.ac.uk; Fax: (+44) 1223-336-017

† Electronic supplementary information (ESI) available: X-Ray data, majority rule study, CD data, ^{13}C NMR data. CCDC reference numbers 743751. For ESI and crystallographic data in CIF or other electronic format see DOI: 10.1039/c0ob00027b

The direction of the helical twist (*M* or *P*) is determined by the chirality at the α-carbon of the constituent amino acid but is independent of the chemical nature of its side chains: an L-amino acid-derived NDI produces a *P*-helix, while a D-amino acid-derived NDI produces an *M*-helix. Due to their chirality the nanotubes may be studied by circular dichroism spectroscopy (Fig. 2).

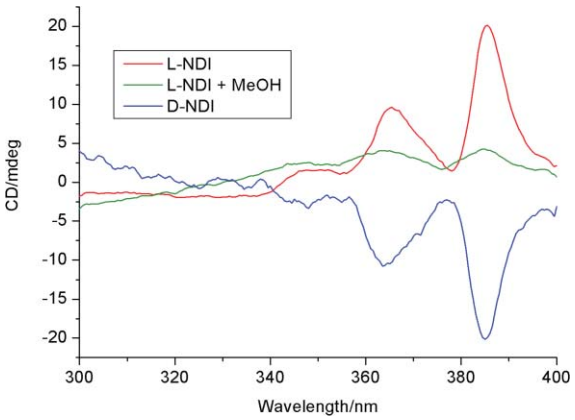

Fig. 2 Example CD traces showing the inverted signal of D-NDI nanotubes with respect to L and the collapse seen when nanotubes are destroyed by the addition of methanol. The NDI used was **1** (see Fig. 4) at a concentration of 1×10^{-3} mol dm^{-3}.

Computational studies have shown that the characteristic CD trace produced by the nanotube helix is due to a dipole–dipole interaction between adjacent NDIs (*i* and *i* + 1) which is strongly dependent on the angle between these naphthyl cores.[6] As expected, the CD trace of a *P*-helix is inverted with respect to that of an *M*-helix. The nanotubes may be destroyed by heating or by adding a polar solvent such as methanol. These actions result in the collapse of the CD signal (see Fig. 2), showing how CD spectroscopy may be used as an indicator of the presence or absence of a nanotube helix. Esterifying the NDI carboxylic acid groups prevents hydrogen bonding and inhibits nanotube formation. Solutions of the esters give similar CD traces to those of the acids plus methanol.

The nanotubes have been found to be an effective receptor for a number of guests. C_{60}, with a diameter of 10.3 Å, is readily taken up into the 12.4 Å interior cavity of the nanotube. The nanotubes are capable of solvating C_{60} in solvents where the fullerene alone has poor solubility, such as chloroform. An observed induced Cotton effect on the C_{60} absorbances indicates that C_{60} senses the chirality of the nanotubes. Most relevantly for the work presented here, the ring current of the naphthyl cores of the NDIs acts to shield the C_{60} carbons, producing a significant upfield shift in their ^{13}C NMR signal (Fig. 3).[7]

Recently, the nanotubes have also been shown to be effective receptors for many aromatic molecules, with a strong dependence on size due to the limits of the interior cavity. More surprisingly, they can also serve as hosts for a wide variety of ions, including those which form donor–acceptor complexes either with or within the nanotube itself.[8,9]

As C_{70} has the same diameter as C_{60}, it was expected that C_{70} would be complexed in a similar fashion by the nanotube. The reality proved to be quite different: addition of C_{70} causes

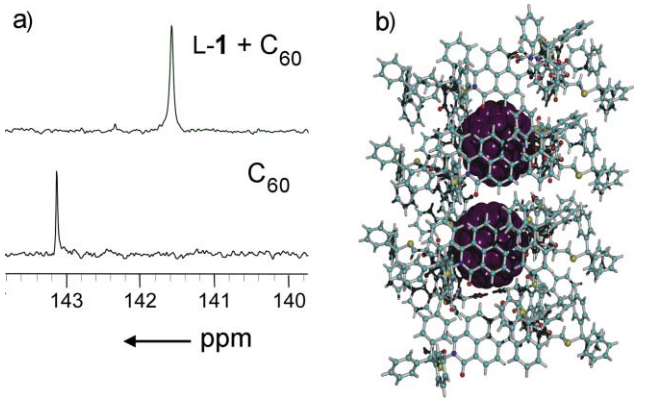

Fig. 3 (a) C_{60} ^{13}C NMR upfield shift of 1.4 ppm observed upon the addition of NDI **1**; (b) computer modelling of C_{60} inside the nanotube cavity, adapted from ref. 3

the destruction of the nanotube and templates the formation of a hexameric NDI 'capsule'-like receptor for individual C_{70} molecules.[10]

Some chiral self-assembling systems are able to incorporate enantiomers of opposite chirality because the chiral centre is relatively remote from the moiety that is involved in self-assembly.[11,12] By contrast, NDI monomers are highly discriminating when it comes to the formation of chiral nanotubes: one enantiomer cannot be incorporated into a helix made of the other enantiomer because the directionality created at the chiral centre is critical to self-assembly. Therefore, when mixed, the two enantiomers self-sort. This is shown by the observation that a 1 : 1 mixture of L-**1** and D-**1** continues to show good receptor behaviour for C_{60}, indicating that nanotubes are still present (even though they are not visible by CD due to the equal proportions of L- and D-enantiomers). The high degree of self-sorting is also shown by a 'majority rules' study[12–14] (see ESI†). Sergeants-and-soldiers behaviour therefore requires that L- and D-enantiomers do not reject an achiral NDI as they would one another.

The sergeants-and-soldiers effect

The 'sergeants-and-soldiers' effect was first proposed in the field of polymer chemistry in the 1960s and was named by M. M. Green and co-workers in 1989.[1,15] Since that time, E. W. Meijer and others have broadened the scope of the concept to take in many facets of supramolecular as well as polymer chemistry.[16–19] In a system with 'sergeants-and-soldiers' behaviour a chiral derivative (the 'sergeant') imposes its chirality on a structure formed mainly out of achiral derivatives, the 'soldiers'. Many systems of this type have been reported.[17,20a–e]

In the case of NDI nanotubes, investigating the possibility of a sergeants-and-soldiers effect requires the synthesis of carboxylate-functionalised NDIs from achiral amino acids. Glycine is perhaps the most obvious choice, but the resulting NDI had previously been found to be highly insoluble in organic solvents. Several different achiral amino acids outside the 'natural 20' were therefore employed to synthesise a range of achiral NDIs.

In this work, we have used chiral NDIs derived from S-trityl cysteine (**1** and control ester **2**), or N-Boc lysine (**3** and control ester **4**) as the sergeant, while achiral derivatives **5–8** were used as soldiers (Fig. 4). For reasons that will become clear below, most

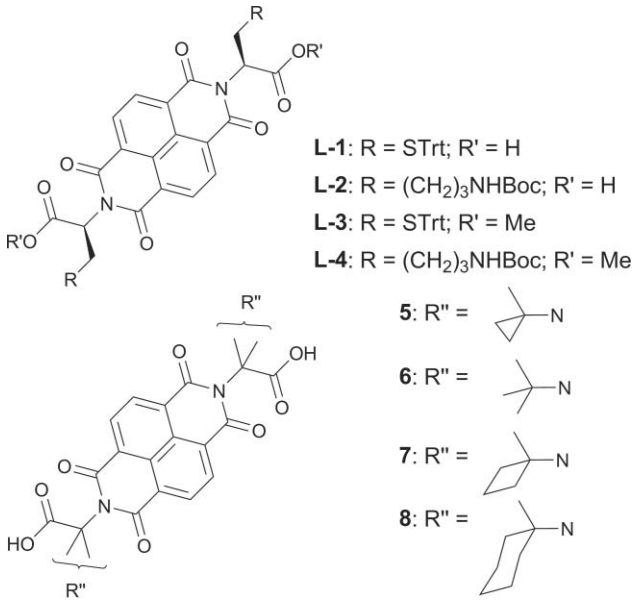

Fig. 4 Chiral NDIs **1** and **2** derived from protected cysteine and lysine, respectively; esterified inactive variants **3** and **4** for control experiments; achiral NDIs **5**, **6**, **7** and **8** derived from the corresponding achiral amino acids (Trt = trityl, Boc = *tert*-butyloxycarbonyl-).

efforts have been focused on NDI **5**. The synthesis of this derivative followed the published procedures,[1] producing **5** in good yield. Crystals of derivative **5** suitable for X-ray diffraction study were obtained from DMSO. In this hydrogen bond acceptor solvent, the NDIs are arranged in a π-stacking structure, with the NDI cores *n* and *n* + 1 tilted at *ca.* 30° with respect to each other, while *n* and *n* + 2 are parallel to each other (dihedral angle 0.6°, Fig. 5).

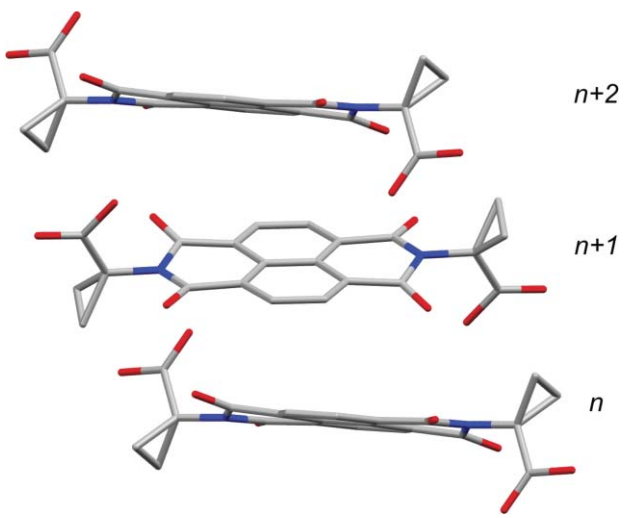

Fig. 5 Crystal structure of **5** showing tilt of NDI *n* + 1 with respect to parallel NDIs *n* and *n* + 2. Note that this is only part of the unit cell; see Experimental Section for details.

Compound **5** is much less soluble than chiral NDIs **1** and **2** in chloroform, but it can be solubilised by heating or by adding protic solvents to break up the π-stacked/hydrogen-bonded structures that may be formed. 1,1,2,2-Tetrachloroethane (TCE) was found to be a superior solvent to chloroform for the achiral NDI. Binding experiments with C_{60} (*vide infra*) in both solvents indicate that these structures are different from the nanotubes observed for the chiral derivatives.

Results and discussion

In order to test the 'sergeants-and-soldiers' effect in the NDI nanotube system, solutions of L-**1** and **5** (2.1×10^{-4} mol dm^{-3} each) were prepared in TCE. Chiral amplification and propagation experiments were performed by addition of L-**1** to a solution of **5** and addition of **5** to solutions of L-**1**, respectively (see Experimental Section for details). Both experiments were then repeated with a solution of the non-hydrogen bonding ester L-**3** substituted for **5** to act as a control. The overall concentration of NDI moieties therefore remains constant throughout the additions. An example of the CD traces across the full scanning range taken for one experiment is shown in Fig. 6(a). The CD_{max} points were then collated and plotted against percentage of L-**1** present to produce Fig. 6(b).

It is immediately clear that the presence of **5** amplifies the CD signal relative to that which the dilute solution of L-**1** can

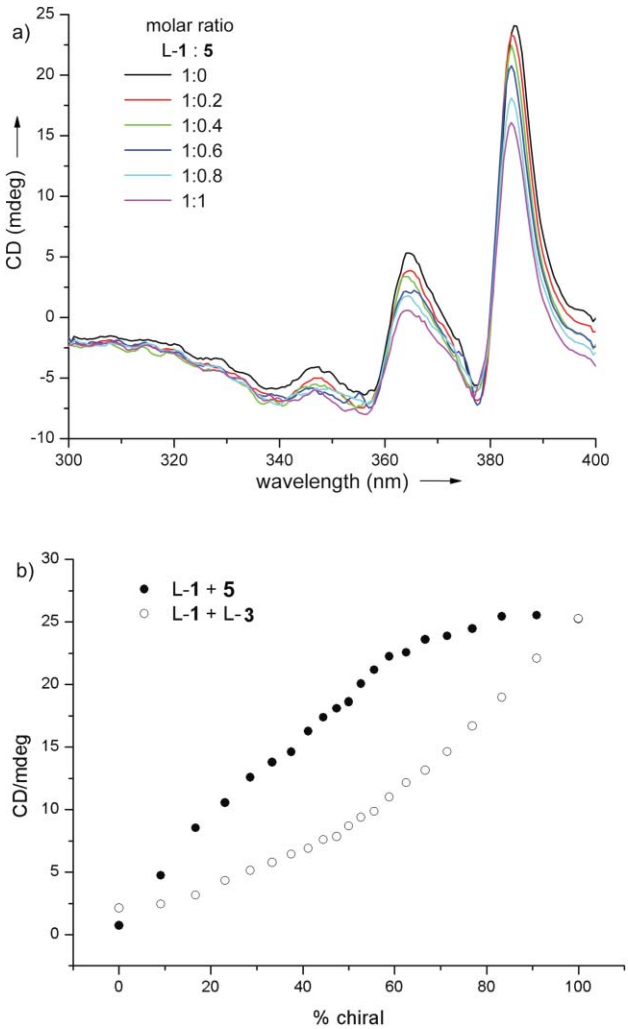

Fig. 6 (a) Overlaid CD traces across the full scanning range for a typical propagation experiment, **5** being added to L-**1**. (b) Plotted CD_{max} (383.5 nm) for all experiments. Concentration of all NDIs = 2.1×10^{-4} mol dm^{-3}.

produce alone. In the centre of the plot, the ratio of L-**1** to **5** is 1 : 1. Maximum amplification (2.5-fold) is observed around 30% L-**1**. Since nanotubes are clearly formed in the presence of as little as 10% chiral NDI,[21] the effective heterogeneous nanotubes' association constant must be at least 10^5 mol^{-1} dm^3; given that the equilibrium constant for carboxylic acid hydrogen bonding in TCE is only of the order of 10^3, this confirms that there is cooperative binding between the NDI monomers, as in homogeneous nanotubes.[2] The curvature of both the 'sergeants-and-soldiers' and control plots in Fig. 6(b), which is also observed even in simple dilution experiments of solutions of nanotubes is likely to be due to the cumulative and cooperative nature of the hydrogen bonding.

A further experiment with the same protocol was used to test that the 'sergeants-and-soldiers' behaviour was not unique to L-**1**. Separate solutions of NDIs D-**2** and L-**2** were each diluted with **5** and with the appropriate ester (D-**4** or L-**4**) as control. When plotted on one graph (Fig. 7) this also illustrates that—as expected—achiral **5** amplifies both *M*- and *P*-helices equally, with no intrinsic preference.

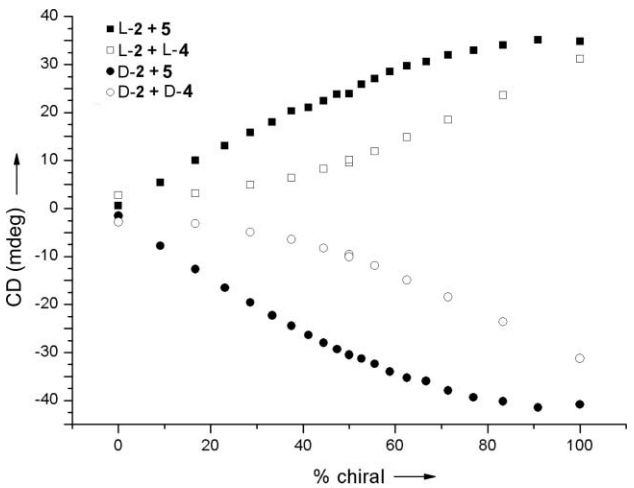

Fig. 7 Plotted CD_{max} points for mixtures of L-**2**/**5** (■) or L-**2**/esterified L-**4** (□); and D-**2**/**5** mixtures (●) or D-**2**/esterified D-**4** (○). Concentration of all NDIs = 2.1×10^{-4} mol dm^{-3}.

C_{60} Studies

As described above, homogenous nanotubes, such as those composed entirely of L-**1**, are known to take up C_{60}. Experiments were performed using ^{13}C NMR in deuterated TCE to study if this functional behaviour is the same for heterogeneous nanotubes made up of a mixture of chiral L-**1** and achiral **5**. NDI solutions of several different ratios of L-**1** to **5** were allowed to stand over C_{60} for 3 h, after which the resulting solution was analysed by ^{13}C NMR. Control experiments were also performed with solutions containing 100% L-**1**, 100% **5**, and C_{60} alone in deuterated TCE to provide 'goalposts' delineating the extreme possibilities. The chemical shifts of the C_{60} peak were then compared as shown in Fig. 8.

The magnitude of the upfield shift of the C_{60} chemical shift, caused by shielding by the ring currents of the naphthalene system and/or adjacent fullerenes, decreases slightly as the proportion

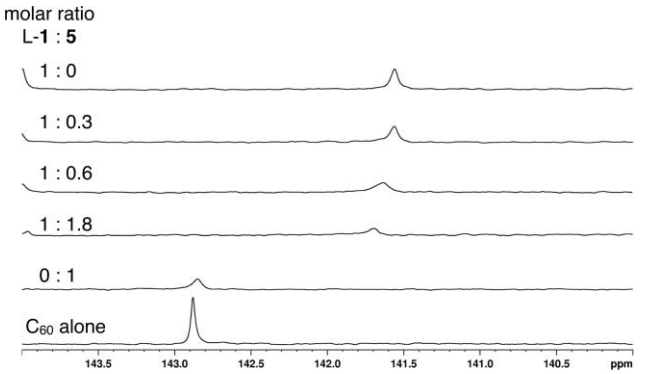

Fig. 8 ^{13}C NMR (125 MHz, 298 K, TCE-d_2) traces of the C_{60} peak; ratio of L-**1** to **5**. Molar ratio NDI : C_{60} is 4 : 1, [NDI] = 7.21×10^{-2} mol dm^{-3}.

of **5** rises. However, even nanotubes composed of more **5** than L-**1** (fourth trace, Fig. 8) still lead to an upfield shift far greater than could be achieved by the quantity of L-**1** present alone. The peak represents a weighted average of C_{60} inside and outside the nanotube, an exchange which is fast on the NMR timescale. The loss of intensity results from a fast exchange between rapidly relaxing bound C_{60} and the slow relaxing free C_{60}. These results therefore indicate that heterogeneous nanotubes become slightly poorer receptors for C_{60} as the proportion of achiral NDI **5** rises.

This may suggest that the superstructure of the heterogeneous nanotubes is subtly different to that of the homogenous L-**1** nanotube. This difference could be due to the achiral **5** lacking the usual amino acid α-proton. The steric repulsion of two alkyl groups on **5** is balanced by the cyclopropyl ring holding them tightly together, meaning the N–C–C(O) angle in **5** is within the range of those of **1** and **2**, both of which readily form nanotubes with similar binding properties (Fig. 9). However the added rigidity imposed by the cyclopropyl moiety forces **5** to take up conformations that are slightly different to the minimum energetic conformation for the chiral amino acid-derived NDIs (which present the α-proton in the most sterically crowded position).

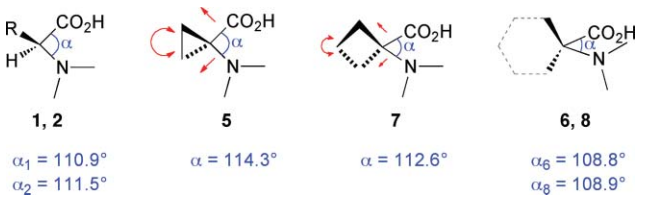

Fig. 9 Ring strain in NDI **5** counteracts the repulsion of the alkyl carbons to bring the N–C–C(O) angle back within the range of an NDI derived from a chiral amino acid with only one R group (**1**,**2**). The lesser ring strain in **7** produces a reduced version of this effect, while it is not present at all in unstrained **6** or **8**. The degree of difference in the N–C–C(O) angle is exaggerated for clarity in the diagrams. Where crystal structures of the NDIs were not available, estimates have been made by averaging the values found in crystal structures of related compounds from CSD.[22]

It is notable that **5** (and **7**) alone does not induce a shift of the peak due to dissolved C_{60} in pure solvent, strikingly suggesting that **5** cannot form a racemic mixture of helical nanotubes.

Other achiral NDIs

The importance of **5**'s three-membered ring strain is demonstrated by the fact that achiral NDIs **6** and **8** derived from achiral amino acids without this strain (Fig. 4) were observed to have no significant sergeants-and-soldiers activity, apparently interacting no more with chiral NDI L-**1** than the control ester does (see ESI†).

Based on this interpretation, we might naively expect an achiral NDI possessing an N–C–C(O) angle somewhere between that of the strained **5** and unstrained **6** and **8** to be a soldier but a poorer one than **5**. Such an achiral NDI is **7**, which is derived from 1-aminocyclobutane-1-carboxylic acid. A four-membered ring naturally has internal angles of 90° rather than the 60° of a three-membered ring, which commensurately means less counteraction of the repulsion compression of the N–C–C(O) angle but some degree remains, unlike the unstrained internal angles of **6** and **8** (Fig. 9).

NDI **7** was found to indeed act as a 'soldier', but an inferior one to **5**, as predicted (Fig. 10). A similar behaviour was observed in the C_{60} complexation studies in which **7** was used as counterpart for L-**1** (see ESI†). This supports the idea that bond angle must be key to the molecule's suitability as a soldier: it is the only significant molecular distinction between NDIs **5**, **6** and **7**, yet accounts for their very variant properties. It may be that future molecular modelling studies will help elucidate the exact consequences of changing the bond angle upon the structure of the hybrid nanotube, and whether a hybrid nanotube can form at all.

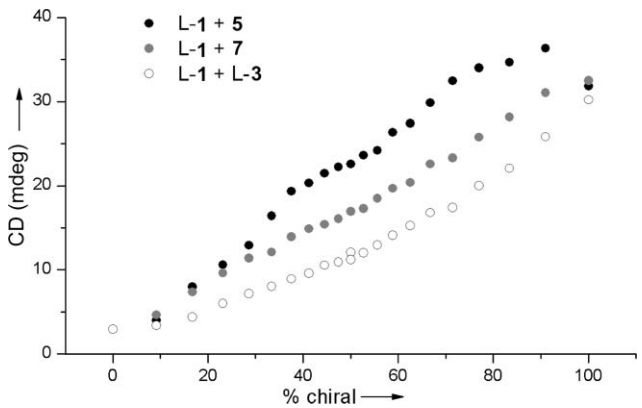

Fig. 10 Example datasets for NDIs **5** (black points) and **7** (grey points) acting as soldiers to L-**1** as sergeant, collected using the same solution of L-**1** to reduce experimental errors. Control data using L-**3** as ester as inactive soldier is also plotted (hollow points). Concentration of all NDIs = 2.1×10^{-4} mol dm^{-3}. Note the black L-**1** + **7** trace has a larger CD signal at 90% chiral than at 100%.

It is notable in Fig. 6, 7, and 10 that solutions of chiral NDIs **1** and **2** containing small percentages of **5** tend to show stronger CD signals than 100% chiral solutions of the same total NDI concentration. The effect is small but reproducible, and must result from a subtly different geometry modifying the size of the exciton coupling between adjacent chromophores.[6] A modified geometry present in the hybrid nanotubes might also explain the inferior C_{60} receptor ability.

Conclusions

A new 'sergeants-and-soldiers' supramolecular system is presented. Chiral amplification behaviour is observed with different chiral NDI 'sergeants' and equally with both enantiomers. An achiral NDI does not form functional nanotubes alone, yet builds upon existing ones. A negative result with other achiral NDIs highlights the high specificity with which NDI monomers may be incorporated into the nanotube. Uptake of C_{60} suggests that the structure of these resulting heterogeneous nanotubes is subtly different and depends on the "soldier" NDI used.

Experimental

General methods

All solvents were of reagent grade quality (DMF, CH_3CN) or HPLC grade ($CHCl_3$) and purchased commercially. All starting materials were purchased from Aldrich and ChemImpex and used without further purification. Melting points were determined with a Gallenkamp apparatus and are uncorrected. NMR spectra were recorded on Bruker DRX 400 MHz or 500 MHz instruments. The NMR spectra were referenced to solvent and the spectroscopic solvents were purchased from Euriso-Top (C. E. Saclay). All the spectra were recorded at 298 K. ^{1}H NMR data are reported as follows: chemical shift in ppm on the δ scale, integration, multiplicity (s: singlet, d: doublet, t: triplet, q: quartet, dd: doublet of doublets, bs: broad singlet, bt: broad triplet), coupling constants (Hz) and assignment. All high-resolution (HR) electrospray ionization mass spectra were recorded on a Waters LCT Premier XE instrument. The sonication was performed using a Bransonic 1210E tabletop ultrasonic cleaner. The microwave experiments were conducted using a CEM Discover™ Microwave Synthesizer. The CD analyses were performed on an Applied Photophysics Chirascan circular dichroism spectrometer. Compounds L-**1**, L-**2**, D-**2**, L-**3**, L-**4** and **8** were synthesized using previously reported methods.[1]

Synthesis of achiral NDI (5)

1,4,5,8-Naphthalenetetracarboxylic dianhydride (200 mg, 0.746 mmol) and 1-aminocyclopropane-1-carboxylic acid (151 mg, 1.494 mmol) were suspended in 6 mL of DMF in a pressure-tight 8 mL microwave vial. To this suspension was added 0.2 mL of dry Et_3N. The suspension was sonicated until the mixture became homogenous. The reaction mixture was heated for 5 min at 140 ± 5 °C (direct flask temperature measurement) under microwave irradiation using a dedicated microwave system. The solvent was removed under reduced pressure, and the reaction mixture was worked-up by being re-dissolved in EtOH (~5–10 mL) and poured into constantly stirred acidified water (5 mL 37% aqueous HCl in 500 mL water). This was allowed to stir at room temperature for a further 1 h, then filtered under suction, the product was collected as a tan solid. The product was thoroughly dried under reduced pressure.

In most cases the product was obtained without need for purification, with a yield averaging 91%. In rare cases requiring purification due to the presence of starting materials or mono-substituted side products, the product was recrystallised from hot chloroform–methanol (7 : 3 ratio). Unreacted NDA did not

dissolve and was filtered from the hot mixture; the mono-substituted side product crystallised out first, allowing separation from the desired di-substituted product, **5**.

Synthesis of other achiral NDIs

The procedure followed was identical to that for **5**, with the exception that the respective achiral amino acid was used in the appropriate quantity (for **6**, 2-aminoisobutyric acid; for **7**, 1-aminocyclobutane-1-carboxylic acid). The synthesis of **7** produces a similar yield as **5** (average 89%) and also rarely requires purification; **6** and **8** have smaller yields (50–60%) and almost always require purification by the method quoted above.

Characterisation data

5. (1,1′(1,3,6,8-tetraoxobenzo[lmn][3,8]phenanthroline-2,7-(1*H*,3*H*, 6*H*,8*H*)-diyl)dicyclopropanecarboxylic acid): mp > 300 °C; ^{1}H NMR (400 MHz, DMSO-d_6) δ (ppm): 12.80 (bs, 2H), 8.70 (s, 4H), 1.81 (dd, J = 2.9, 4H), 1.47 (t, J = 2.9, 4H); ^{13}C NMR (1H) (100.62 MHz, DMSO-d_6) δ (ppm): 172.5, 163.2, 131.1, 126.7, 35.2, 18.7; HRMS (ESI+) calcd for: $C_{22}H_{15}N_2O_8$ [M + H]$^+$ (m/z): 435.0828, found: 435.0847; Elemental analysis for $5C_{22}H_{14}N_2O_8{\cdot}1H_2O$, calcd: C 60.28%, H 3.40%, N 6.39%, found C 60.13%, H 3.29%, N 6.30%.

6. (2,2′(1,3,6,8-tetraoxobenzo[lmn][3,8]phenanthroline-2,7-(1*H*,3H, 6*H*,8H)-diyl)bis(2-methylpropanoic acid): mp > 300 °C; ^{1}H NMR (400 MHz, DMSO-d_6) δ (ppm): 12.57 (bs, 2H), 8.63 (s, 4H), 1.83 (s, 6H); ^{13}C NMR (1H) (100.62 MHz, DMSO-d_6) δ (ppm): 174.3, 164.13, 127.63, 126.40, 63.50, 25.19; HRMS (ESI+) calcd for: $C_{22}H_{19}N_2O_8$ [M + H]$^+$ (m/z): 439.1141 found: 439.1136; Elemental analysis for $3C_{22}H_{18}N_2O_8{\cdot}2H_2O$, calcd: C 58.67%, H 4.33%, N 6.22%, found: C 58.76%, H 4.21%, N 6.26%.

7. (1,1′(1,3,6,8-tetraoxobenzo[lmn][3,8]phenanthroline-2,7-(1*H*,3*H*,6*H*,8H)-diyl)dicyclobutanecarboxylic acid): mp > 300 °C; ^{1}H NMR (400 MHz, DMSO-d_6) δ (ppm): 13.08 (bs, 2H), 8.65 (s, 4H), 2.86 (dd, J_1 = 9.1, J_2 = 10.0, 2H), 2.71 (dd, J_1 = 9.1, J_2 = 10.0, 2H), 2.27 (dd, J_1 = 9.6, J_2 = 10.0, 1H), 1.82 (dd, J_1 = 9.6, J_2 = 10.0, 1H); ^{13}C NMR (1H) (125 MHz, TCE-d_2) δ (ppm): 161.60, 143.90, 129.41, 127.92, 126.80, 126.14, 67.48, 52.50, 45.72; HRMS (ESI+) calcd for: $C_{24}H_{19}N_2O_8$ [M + H]$^+$ (m/z): 463.1141 found: 463.1136; Elemental analysis for $4C_{24}H_{18}N_2O_8{\cdot}1H_2O$, calcd: C 61.66%, H 4.00%, N 6.04%, found C 61.65%, H 4.05%, N 6.19%.

X-Ray crystallography of 5

Achiral NDI **5** was crystallised from dimethylsulfoxide solution at room temperature (Fig. 11). Under such conditions **5** was found to form a monoclinic unit cell with space group $P2_1/c$. Unit cell dimensions: a = 9.0612(2); b = 11.8489(2); c = 28.6964(5) Å; volume = 3047.05(10) Å^3. Further details may be found in the ESI.†

CD experimental procedures

A solution of **5** (or another achiral NDI) in 1,1,2,2-tetrachloroethane (TCE) at the required concentration was heated to 100 °C for 1 h with stirring, to aid solubilisation. The solution of **5** was allowed to cool to room temperature. (Tests have shown that such a solution is experimentally viable for over 5 h at room temperature without reheating, significant precipitation only occurring after more than 16 h). Solutions of the same concentration of the required chiral NDIs were prepared in TCE.

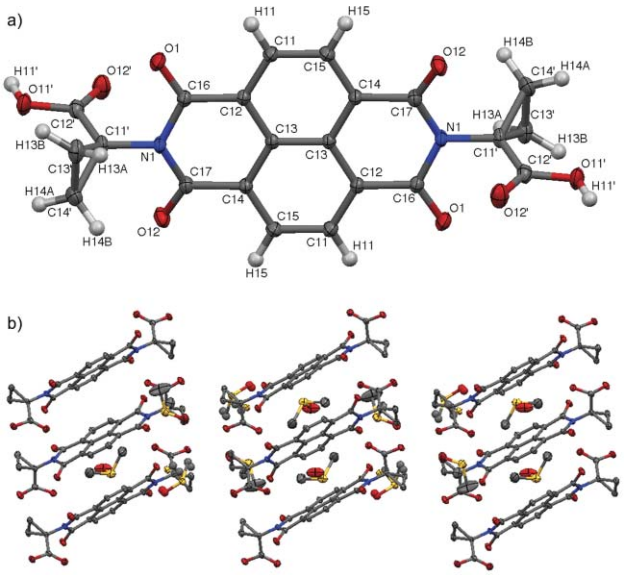

Fig. 11 (a) Molecular structure of **5** showing the atom labelling scheme. Displacement ellipsoids are scaled to the 50% probability level; b) Unit cell packing diagram for single crystals of **5**.

Quartz cuvettes of path length 5 mm and 10 mm were used (volume of 2 mL and 4 mL, respectively) for all experiments. An example of a full data run from 100% chiral to 100% achiral was recorded as follows, using a 5 mm, 2 mL cuvette with chiral NDI L-**1** and achiral NDI **5** (as seen in Fig. 6(b)). 1 mL of the L-**1** solution was added to the cuvette and the CD signal recorded from 400 to 270 nm three times, smoothed and averaged. 0.1 mL of a solution of **5** of equal concentration was added, the cuvette shaken and allowed to stand for 1 min, and the signal again recorded by the same procedure. This was repeated until the cuvette was filled and had therefore reached 50% achiral/50% chiral. The whole experiment was then repeated three times and the results averaged to minimise experimental error. The averaged CD_{max} points of each recording were plotted against percentage chiral NDI present. This provides the 100–50% chiral part of the data run covering the right side half of Fig. 6(b). A second experiment was then performed using the same procedure, but this time starting with achiral **5** and then adding 0.1 mL volumes of chiral L-**1** until 50% achiral/50% chiral was reached, and this too was repeated three times, averaged and the CD_{max} points plotted. This provides the 50–100% achiral part of the data run covering the left side half of Fig. 6(b). Finally the experiments were performed again (only a single time) using H-bond-inactive ester L-**3** instead of **5** to provide the control data.

The results shown in Fig. 7 were obtained by the same procedure, except now using L-**2** and D-**2** as the chiral NDIs in question, and L-**4** and D-**4** for the control esters. Raw CD data plots are shown in the ESI.†

^{13}C NMR experimental procedures (C_{60} uptake study)

Mixtures of NDIs L-**1** and **5** were made up in the following proportions: 1 : 0, 1 : 3, 1 : 1, 3 : 1 and 0 : 1. The total molar content

of each sample was 11.12 mmol. Each sample was dissolved in 2.5 mL of 1,1,2,2-tetrachloroethane-d_2 and allowed to stand over excess C_{60} for 4 h. A control vial containing only solvent and C_{60} was also made up. 0.7 mL of each mixture was then transferred to an NMR tube and ^{13}C NMR was taken using a Bruker Avance 500 TCI spectrometer. Data for each nanotube fullerene complex was acquired over 800 scans with a delay of 6 s. The peaks in the ^{1}H NMR spectra were integrated and the ratio of L-**1** to **5** recalculated from this to take any precipitation into account.

Acknowledgements

We thank Pembroke College, Cambridge, and EPSRC for financial support and Dr J. E. Davies for the X-ray crystal structure of **5**.

Notes and references

1 M. M. Green, M. P. Reidy, R. J. Johnson, G. Darling, D. J. Oleary and G. Willson, *J. Am. Chem. Soc.*, 1989, **111**, 6452.
2 P. Pengo, G. D. Pantoş, S. Otto and J. K. M. Sanders, *J. Org. Chem.*, 2006, **71**, 7063.
3 G. D. Pantoş, P. Pengo and J. K. M. Sanders, *Angew. Chem., Int. Ed.*, 2007, **46**, 194.
4 F. Wurthner and S. Yao, *Angew. Chem., Int. Ed.*, 2000, **39**, 1978.
5 F. Wurthner, C. Thalacker, S. Diele and C. Tschierske, *Chem.–Eur. J.*, 2001, **7**, 2245.
6 B. M. Bulheller, G. D. Pantoş, J. K. M. Sanders and J. D. Hirst, *Phys. Chem. Chem. Phys.*, 2009, **11**, 6060.
7 G. D. Pantoş, J. L. Wietor and J. K. M. Sanders, *Angew. Chem., Int. Ed.*, 2007, **46**, 2238.
8 E. Tamamini, G. D. Pantoş and J. K. M. Sanders, *Chem.–Eur. J.*, 2010, **16**, 81.
9 E. Tamanini, N. Ponnuswamy, G. D. Pantoş and J. K. M. Sanders, *Faraday Discuss.*, 2010, **145**, 205.
10 J. L. Wietor, G. D. Pantoş and J. K. M. Sanders, *Angew. Chem., Int. Ed.*, 2008, **47**, 2689.
11 A. R. A. Palmans and E. W. Meijer, *Angew. Chem., Int. Ed.*, 2007, **46**, 8948.
12 (*a*) M. M. J. Smulders, I. A. W. Filot, J. M. A. Leenders, P. van der Schoot, A. R. A. Palmans, A. P. H. J. Schenning and E. W. Meijer, *J. Am. Chem. Soc.*, 2010, **132**, 611; (*b*) M. M. J. Smulders, P. J. M. Stals, T. Mes, T. F. Paffen, A. P. H. J. Schenning, A. R. A. Palmans and E. W. Meijer, *J. Am. Chem. Soc.*, 2010, **132**, 620.
13 J. Van Gestel, *Macromolecules*, 2004, **37**, 3894.
14 J. Van Gestel, A. R. A. Palmans, B. Titulaer, J. A. J. M. Vekemans and E. W. Meijer, *J. Am. Chem. Soc.*, 2005, **127**, 5490.
15 C. Carlini, F. Ciardelli and P. Pino, *Makromol. Chem.*, 1968, **119**, 244.
16 (*a*) A. R. A. Palmans, J. A. J. M. Vekemans, E. E. Havinga and E. W. Meijer, *Angew. Chem., Int. Ed. Engl.*, 1997, **36**, 2648; (*b*) L. Brunsveld, B. G. G. Lohmeijer, J. A. J. M. Vekemans and E. W. Meijer, *Chem. Commun.*, 2000, 2305; (*c*) R. B. Prince, J. S. Moore, L. Brunsveld and E. W. Meijer, *Chem.–Eur. J.*, 2001, **7**, 4150.
17 S. J. George, Z. Tomovic, M. M. J. Smulders, T. F. A. de Greef, P. E. L. G. Leclere, E. W. Meijer and A. P. H. J. Schenning, *Angew. Chem., Int. Ed.*, 2007, **46**, 8206.
18 (*a*) M. M. J. Smulders, A. P. H. J. Schenning and E. W. Meijer, *J. Am. Chem. Soc.*, 2008, **130**, 606; (*b*) T. F. A. de Greef, M. M. J. Smulders, M. Wolffs, A. P. H. J. Schenning, R. P. Sijbesma and E. W. Meijer, *Chem. Rev.*, 2009, **109**, 5687; (*c*) M. M. J. Smulders, M. M. L. Nieuwenhuizen, T. F. A. de Greef, P. Van Der Schoot, A. P. H. J. Schenning and E. W. Meijer, *Chem.–Eur. J.*, 2010, **16**, 362.
19 A. J. Wilson, M. Masuda, R. P. Sijbesma and E. W. Meijer, *Angew. Chem.*, 2005, **117**, 2315.
20 (*a*) J. C. Nelson, J. G. Saven, J. S. Moore and P. G. Wolynes, *Science*, 1997, **277**, 1793; (*b*) R. B. Prince, T. Okada and J. S. Moore, *Angew. Chem., Int. Ed.*, 1999, **38**, 233; (*c*) M. L. Bushey, A. Hwang, P. W. Stephens and C. Nuckolls, *Angew. Chem., Int. Ed.*, 2002, **41**, 2828; (*d*) S. R. Nam, H. Y. Lee and J.-I. Hong, *Chem.–Eur. J.*, 2008, **14**, 6040; (*e*) D. Monti, M. De Rossi, A. Sorrenti, G. Laguzzi, E. Gatto, M. Stefanelli, M. Venanzi, L. Luvidi, G. Mancini and R. Paolesse, *Chem.–Eur. J.*, 2010, **16**, 860.
21 In a mixture containing 10% L-**1** and 90% **5** about 20% of the NDI material is assembled into nanotubes. In the control experiment containing 10% L-**1** and 90% L-**3** only about 10% of the NDI material is assembled in nanotubes.
22 Cambridge Structural Database, v.5.30, 2009.

